Applied Nanoscience (2018) 8:1069–1090
https://doi.org/10.1007/s13204-018-0746-4

ORIGINAL ARTICLE

Experimental study of improved rheology and lubricity of drilling fluids enhanced with nano-particles

O. Anwar Bég[1] · D. E. Sanchez Espinoza[2] · Ali Kadir[1] · MD. Shamshuddin[3] · Ayesha Sohail[4]

Received: 29 January 2018 / Accepted: 26 March 2018 / Published online: 5 April 2018

Abstract

An experimental study of the rheology and lubricity properties of a drilling fluid is reported, motivated by applications in highly deviated and extended reach wells. Recent developments in nanofluids have identified that the judicious injection of nano-particles into working drilling fluids may resolve a number of issues including borehole instability, lost circulation, torque and drag, pipe sticking problems, bit balling and reduction in drilling speed. The aim of this article is, therefore, to evaluate the rheological characteristics and lubricity of different nano-particles in water-based mud, with the potential to reduce costs via a decrease in drag and torque during the construction of highly deviated and ERD wells. Extensive results are presented for percentage in torque variation and coefficient of friction before and after aging. Rheology is evaluated via apparent viscosity, plastic viscosity and gel strength variation before and after aging for water-based muds (WBM). Results are included for silica and titanium nano-particles at different concentrations. These properties were measured before and after aging the mud samples at 80 °C during 16 h at static conditions. The best performance was shown with titanium nano-particles at a concentration of 0.60% (w/w) before aging.

Keywords Nano-particles · Drilling muds · Rheology · Lubricity · Titanium · Silica · Viscosity · Gel strength · Torque

Introduction

In the oil and gas industry, drilling is a fundamental and expensive operation. The efficient construction of wells involves many stages including measurement while drilling (MWD), logging while drilling (LWD), directional drilling (DD), casing design, cementing, drilling fluids, solid control and maintenance. A key element of the entire drilling process is *drilling fluid engineering* which requires carefully fabricated *drilling fluid* (e.g., muds) which must perform repeatedly many functions at the same time and over long periods (Gray et al. 1980). Drilling fluids (muds) serve to cool and lubricate the drilling bit and other critical features include maintenance of an adequate fluid density, the ability to clean the borehole from drilled cuttings, reducing formation damage (wherein the drilling mud does not achieve sufficient hydrostatic pressure to mitigate formation fluids from entering into the well bore), fluid loss, provision of wellbore stability and creating a mud cake. Although petroleum engineers have developed new methods due to new challenges in the discovery of new hydrocarbon reserves, there remain problems related to the performance of drilling muds. These include pipe sticking, drag and torque increase,

✉ MD. Shamshuddin
shammaths@gmail.com

O. Anwar Bég
O.A.Beg@salford.ac.uk

D. E. Sanchez Espinoza
dese1980@gmail.com

Ali Kadir
a.kadir@salford.ac.uk

Ayesha Sohail
Ayesha1981s@gmail.com

1 Mechanical/Aeronautical Engineering, Salford University, Manchester, England M54WT, UK

2 Petroleum Engineering, 228 Malecón del Salado, Guayacanes y Jiguas, Guayaquil, Ecuador

3 Department of Mathematics, Vaagdevi College of Engineering, Warangal, Telangana, India

4 Department of Mathematics, COMSATS Institute of Information Technology, Lahore 54000, Pakistan

erosion of boreholes, formation consolidation, gel formation and lost circulation. These difficulties, which could delay a continuous operation during drilling, can also result in a huge loss of income for the service companies due to production downtime, waste of material and possibly also environmental hazards. Many strategies have been developed in recent years to improve the resilience and in particular lubrication properties of drilling muds. These generally utilize the addition of additives to the drilling mud which is aimed to modify properties and generate enhanced performance. Dingsøyr et al. (2004) investigated the use of viscosifiers, wetting agents and weighting materials to modify the composition and rheology of drilling fluids. Dantas et al. (2014) studied experimentally the influence of chemical additives including high-viscosity carboxymethylcellulose (HV-CMC), calcite and starch on rheological and filtration properties of inhibited drilling fluids composed by potassium citrate. They found that fluid loss was minimized for drilling fluids comprising starch and calcite in high concentrations, or with starch, HV-CMC, and calcite in high concentrations. Qu et al. (2009) presented laboratory test results for the influence of inhibitive property of polyoxyalkylene amine (POAM) additive in water-based drilling fluids, demonstrating reduced toxicity, an improvement in the inhibition of hydration of Na-MMT and furthermore a reduction in the swelling or hydration of shale cuttings. Ahmet et al. (2013) investigated a variety of chemical commercial lubricants on drilling mud (water-based lignosulfonate) rheology and drilling lubricity using a lubricity tester to evaluate the best lubricity/cost ratio of lubricant compositions, noting that the presence of high chloride ion content leads to reduced efficiency in drilling fluid lubricity and rheology. Further studies addressing the modification in drilling fluid lubricity and flow efficiency have been communicated by Olatunde et al. (2012), Behnamanhar et al. (2014) and Slawomir et al. (2009) and for polymeric gel additives in drilling fluids (Bu et al. 2013).

In the recent years, *nanotechnology* has emerged as a vibrant new development in science and engineering. This involves the manipulation of material properties at the nanoscale. *Nanofluids*, in particular, which are synthesized by the suspension of nano-particles in conventional working fluids (water, oil, mud, coolant, etc.), have yielded considerable improvements in many different applications. Introduced by Choi (1995), nanofluids have been shown to dramatically elevate heat transfer properties (such as thermal conductivity, thermal diffusivity) and via modification in viscosity to improve lubrication performance and heat dissipation in friction processes. Nano-particles have been successfully implemented in medical engineering (Bég et al. 2017), aerospace systems (Kannaiyan et al. 2016), heat exchanger technology (Huminic and Huminic 2012) and solar energy collectors (Kaloudis et al. 2016). With a reduction in fabrication costs and customization of different nano-particles for specific oil fields, nanofluids have recently stimulated some interest in petroleum and gas engineering. (Amanullah et al. 2011) showed that spherical nano-particles introduced in drilling muds can decrease differential pipe sticking by forming a thin film around the borehole wall and furthermore may help to dissolve drilling cuttings which aggregate at the base of horizontal well-drilling pipes. Mostafavi et al. (2011) conducted extensive filtration and rheology tests performed on calcium carbonate and iron hydroxide nano-particles in invert (water/oil) emulsion-drilling fluids, noting the significant capabilities of nano-calcium carbonate to increase the consistency and sealing capabilities of the filter cakes and iron hydroxide nano-particles in reducing fluid losses. Abdo and Haneef (2013) reported on the reduction in drilling problems achieved with clay nano-particles in drilling fluids for deep hydrocarbon wells in Oman. Al-Yasiri and Al-Sallami (2015) identified the benefits of nano-particles in overcoming the shortcomings of conventional water and oil-based drilling fluids (gelation, degradation of weighting materials and breakdown of polymeric additives). Fazelabdolabadi et al. (2015) studied the fabrication of nano-based drilling fluids from water/oil-based fluids using functionalized/unfunctionalized (multi-walled) carbon nanotubes (CNT), showing the influence of volume fraction of CNTs on thermal conductivity, viscosity/yield point, and filtrate amount in all samples. Zakaria et al. (2012) described a new class of nanoparticle loss circulation materials for oil-based drilling fluids noting a considerable decrease in fluid loss with nano-particles, a thinner filter cake which is beneficial for mitigating formation damage during drilling and also minimizing differential pressure sticking and increased stability of the drilling fluid.

In the current work, results based on a number of rheological and lubricity tests for several different nano-particles added to water-based mud are described. The objective is to establish whether a decrease in drag and torque is achievable via nano-particles added to mud which could reduce operational costs in, for example, highly deviated wells. Percentage in torque variation before aging and coefficient of friction before aging are documented. Rheological characteristics are computed via apparent viscosity and gel strength variation before aging. It is concluded that improvement in rheological performance can be achieved and that water-based muds (WBMs) may be modified effectively with different nano-particles for deployment in actual drilling operations. We explore the titanium dioxide and silicon dioxide nano-particles which are used to dope water-based drilling mud. The benefits of these metallic (titanium) and tetravalent metalloid (silicon)-based nano-particles has been well established in many excellent studies in the recent years. These materials have been shown to offer considerable advantages in numerous technological applications including

biomedical (Yang et al. 2015) and energy systems (Yang et al. 2014). Other important studies on nano-particle (e.g., graphene oxide, carbon nanotubes, etc.) influence on solubility, mechanical properties and adhesion include Lvov et al. (2011), Jin et al. (2014) and Tian et al. (2017). The current study is restricted for brevity to the laboratory analysis of only two nano-particles. However, the methodology is extendable to all of these other advanced nano-materials (and other metallic oxides e.g., zinc oxide, copper oxide, silver oxide, etc.) indeed efforts in this regard are continuing at Salford University.

Methodology

Apparatus and materials

The potential of nano-particles in improving drilling mud properties, as testified to by many of the works reviewed in "Introduction", have motivated experiments to be conducted in the Salford University Petroleum Engineering Laboratory using silica and titanium nano-particles. These were aimed to evaluate the performance of a water-based drilling mud with nano-particles at different concentrations, in a lubricity tester to determine if these additives could be used as friction reduction agents. Since coefficient of friction is a function of temperature, each sample was heated up at different temperature intervals to analyse its lubricity and rheology before aging, then, the samples were aged during 16 h in an oven at high temperature to simulate borehole conditions to check for variations in the same parameters. A number of different devices were utilized to quantify properties of the nano-particles and the drilling muds doped with these particles. A Hamilton Beach high-speed mixer was used to provide a homogeneous mixture of fine particles through their mechanical dispersion at a high shear rate of about 11,500 RPM (data retrieved from FANN 2016). It was used to mix the drilling fluid and nano-particles. An Ultrasonic Bath—DAWE (Type 6444 Sonicleaner) apparatus which uses ultrasound waves propagated through water was employed to provide a better dispersion of nano-particles in the WBM. The cavitation phenomenon is used to disperse nano-particles in the drilling mud since it creates bubbles that explode and help to break the formation of clusters in nano-particles. This sonicator was used after mixing the nano-particles in the mixer to prepare the most homogenous mixture possible, as it has been reported that this apparatus reduces the agglomeration of nano-particles (Hwang et al. 2008). An OFITE mud balance device was used to provide a direct reading of the drilling mud density. It has four scales to measure density that are useful for drilling operations: ppg, SP GR (specific gravity), lb/ft^3 (pounds per cubic feet), and PSI/1000 ft (pounds per 1000 feet). The method of operation consists of pouring the drilling fluid into the container, then the lid of the container is placed, and some fluid should pass through the hole of the lid. Then, the mud balance is placed on the base that supports its knife edge and the rider, which act as a counterweight, and is moved across the arm until the bubble of the level vial is in the middle. When equilibrium is achieved, the reading is taken from different scales. Additionally, its accuracy is ± 0.1 ppg or ± 0.01 SP GR (data retrieved from OFITE 2014). An OFITE Model 800 Viscometer, as shown in Fig. 1, was used to measure the rheological properties of drilling fluids applying a constant shear rate and shear stress in the drilling mud. This apparatus provides a direct reading of the viscosity, in centipoise (cp), of the drilling mud through a lighted dial. In addition, it has a speed accuracy of ± 0.1 RPM (data retrieved from OFITE 2014). Via readings obtained at different speeds, some theological parameters can be calculated such as *plastic viscosity*, *yield point*, *apparent viscosity* and *gel strength*. The calculations for the first three of these parameters are made with the following formulae:

- Plastic viscosity (PV):

$$\mathrm{PV} = 600\,\mathrm{RPM\ reading} - 300\,\mathrm{RPM\ reading},\ (\mathrm{cp}) \quad (1)$$

- Yield point (YP):

$$\mathrm{YP} = 300\,\mathrm{RPM\ reading} - \mathrm{PV},\ (\mathrm{lb}/100\,\mathrm{ft}^2) \quad (2)$$

- Apparent viscosity (AV):

$$\mathrm{AP} = \frac{600\,\mathrm{RPM\ reading}}{2},\ (\mathrm{cp}) \quad (3)$$

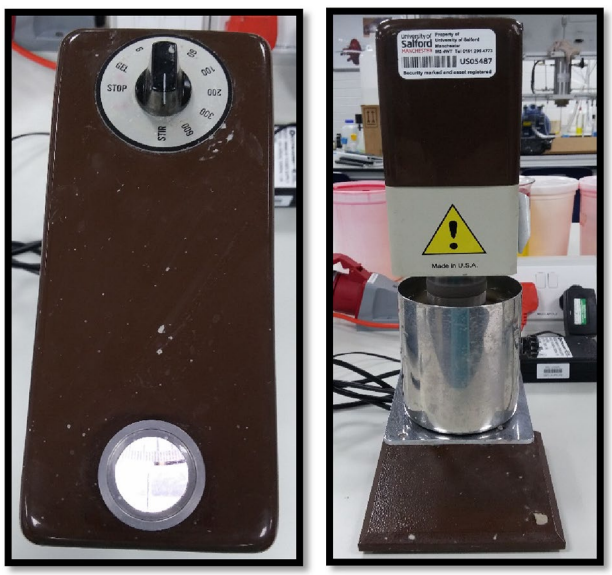

Fig. 1 Viscometer-Model 800 OFITE used in nano-particle experiments

- Gel strength:
  The calculation of the gel strength is taken directly from the dial reading after stopping the apparatus for 10 s and 10 min, and then turning it on at the speed of 3 RPM (the knob is located on the position of gel). It is measured in lb/100 ft^2.

An OFITE oven was employed to simulate static or dynamic aging of the drilling mud in borehole conditions at high temperatures and pressures for long periods. This is useful to simulate the behaviour of drilling fluid at the bottom of the borehole, where temperature and pressure are higher, after the drill string has been removed from the well for a long time due to different operations, such as changing the bit, logging evaluation or placing of a casing section in the well. The oven allows an analysis of the stability of the mud to be performed for realistic working conditions during which the degradation of the fluid is more drastic. A rectification in mud properties may be achieved before running a real operation. The method of operation is simple and it can be programmable. Furthermore, the process of aging is made through an aging cell that keeps the fluid isolated (data retrieved from OFITE 2014). An OFITE lubricity tester (Fig. 2) is also deployed to simulate the increase in torque and pressure of a drill string when it is exposed to a high deviation angle during a well construction. During these operations, the drill string tends to settle down at the lower section of the well path. Hence, a section of the drill string could be in contact with the casing, a rock section or drill cuttings, which lead to an increment in the coefficient of friction (CoF) and decreased lubricity, if the lubricating film is broken.

The lubricity tester measures the lubricity as a function of the CoF of the drilling mud between two solid steel surfaces: a *test ring shaft that turns at a constant speed* and the *concave groove of a block that is located in a torque shaft lever arm*. This lever arm can be adjusted to the desired torque to press both surfaces. The torque arm has a handle that can adjust the torque to a maximum of 600 in.-pounds. Therefore, pressures as high as 100,000 psi can be attained depending on the speed of the ring shaft. The lubricity is measured submerging both, the ring and the block, in a drilling mud sample for a period at a constant speed and torque (of the torque arm). Taking into account that the distance between the centre of the block and torque bushing is 1.5 in. (as it can be observed in Fig. 3), and the standard test is made at 150 in.-pounds, the resulting force applied is 100 lbf. Moreover, a correction factor needs to be applied since the surfaces of both elements are not always the same. Therefore, the CoF is calculated dividing the meter reading and the force generated by the block when pressed against the test ring using the torque arm:

$$\mathrm{CoF} = \frac{\text{Meter reading} \times \text{Correction factor}}{\text{Force of the block against the ring}}. \tag{4}$$

Here:

$$\text{Correction factor} = \frac{\text{Standered meter reading for Deionized water}}{\text{Meter reading obtained in Deionized water calibration}}. \tag{5}$$

Additionally, an SEM was used to analyse the dispersion, morphology and composition of nano-particles in the base mud after aging them. Other devices implemented in the experiments included a hotplate stirrer for heating up the drilling mud samples to the desired temperature, a pH meter for controlling the acidity of the mud samples. Nano-particles utilized for this experiment were titanium oxide (TiO_2), also known as titanium dioxide or titania, and silicon dioxide (SiO_2), also known as silica. Properties are summarized in the Appendix. Both nano-particles were provided by US Research Nanomaterials, Inc. These materials occur naturally and have been used for numerous different applications. They appear due to the normal process of oxidation of the sources where they are found. In the case of titania, which is crystalline, it is found on minerals such as ilmenite, rutile and anatase. The

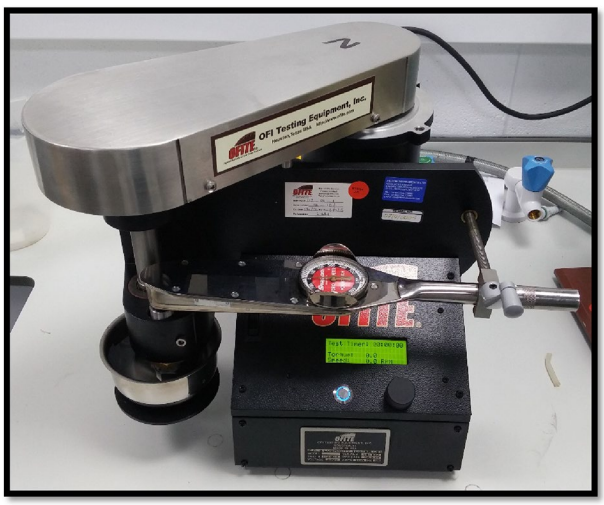

Fig. 2 Lubricity tester (OFI, Houston, Texas, USA)

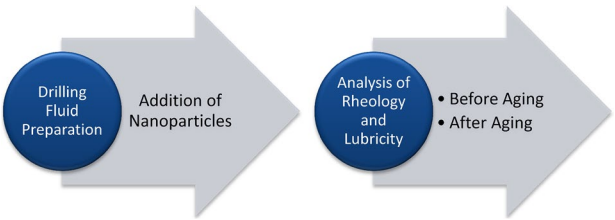

Fig. 3 Experimental procedure

main source of silica is the mineral quartz, although, it can be found in sand as well. Silica is much more abundant than titania. These compounds are categorized as ceramic materials since they are oxides and are, therefore, hard and brittle. However, the implementation of these materials in drilling muds has not been investigated rigorously and this is a major motivation for the present work, in particular with regard to rheology and lubricity in drilling fluids. The silicon dioxide (SiO_2) nano-particles have an amorphous structure and are coated with 3–4% (w/w) KH550 which make them super hydrophilic. The drilling mud used for this experiment was a WBM classified as a low-solids non-dispersed (LSND). This drilling mud was used to compare results before the addition of nano-particles. The additives used were bentonite, barite and xanthan gum. Each of these additives performs different functions in this drilling mud. For instance, bentonite is a material made of clay compounds which swells in the presence of water, so that it is normally used to provide efficient hole cleaning and prevent fluid loss into the formation, moreover, is the most common additive used in WBM. Barite is composed by barium sulphate and it is utilized as a weighting agent to increase the density of the drilling mud. Xanthan gum is a polymer generated by bacteria and it is used to increase the viscosity of drilling fluids when their density is low.

Experimental procedures

The following diagram depicts the four stages to the experiments conducted. First, the drilling mud was prepared using the additives mentioned and its rheology and lubricity was evaluated before and after aging. Then, four mud samples were mixed to add two different concentrations of each of the nano-particles and the same tests were performed on them.

Drilling fluid preparation

1. In the cup of the mixer were added 350 ml of distilled water and 15 g of bentonite. This mixture was stirred for 15 min approximately. It was then left at rest for the same amount of time to allow clay hydration.
2. Next 15 g of Barite were added to increase the density of the fluid, and it was mixed for 5 min.
3. Finally, 0.7 g of xanthan gum were added in small portions to avoid the formation of lumps in the drilling mud and produce a more homogeneous mixture. This was stirred for 10 min and left at rest for the same amount of time (Fig. 4).

Addition of nano-particles

1. After preparing the drilling fluid and left at rest for some time, nano-particles were added to the drilling mud in the following concentrations (Table 1) for each mud sample of 350 ml.
2. Then, the nano-particles were mixed in the drilling fluid using two different two-step methods: stirring and an ultrasonic agitation.
3. When using the mixer, nano-particles were stirred at high speed during 40 min.
4. Soon after, they were introduced in the ultrasonic bath using Erlenmeyer flasks, as it can be observed in the following figure.
5. After 30 min, the ultrasonic bath was stopped and the samples were left to rest at room temperature (Fig. 5).

Analysis of rheology and lubricity before aging

Drilling fluid samples before and after adding nano-particles were evaluated in the same way.

1. After drilling fluid samples were cooled down to 26 °C, density, rheology and lubricity was measured using the mud balance, viscometer and lubricity tester, respectively.
2. The rheology was measured observing a stable value in the dial reading at 600, 300, 200, 100, 60, 30 and 6 RPM. Gel strength was measured observing the maximum deflection in the dial reading at 3 RPM when the viscometer was turned on at this speed after the mud sample was left at rest for 10 s and 10 min.

Table 1 Nano-particle concentrations

Nano-particles	Concentration (w/w %)
TiO_2	0.20
	0.60
SiO_2	0.20
	0.60

Fig. 4 Drilling fluid preparation

Fig. 5 Addition of nano-particles in the drilling fluid

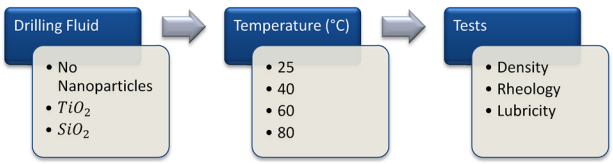

Fig. 6 Analysis performed before aging

3. The lubricity test was carried out calculating the correction factor for the lubricity ring and lubricity block and observed each minute during 6 min.
4. Then, the fluid samples were heated up in the hotplate stirrer at 40, 60 and 80 °C, and the same tests were performed to simulate the mud samples behaviour during drilling operations (Fig. 6).

Analysis of rheology and lubricity after aging

1. The drilling fluid samples (with and without nano-particles) were poured into aging cells.
2. Then, they were placed in the oven for 16 h at 80 °C. The samples remained static during this period to simulate bottom hole conditions.
3. After this time, the samples were cooled down to 26 °C and its rheology was evaluated. Then, the samples were stirred in the mixer for 10 min and its rheology was tested again, as well as its lubricity using the same procedure for the samples before aging.

In addition, during the drilling fluid preparation, the pH level of the mixture was continuously checked with the pH meter to maintain it at 10 via the addition of caustic soda (Figs. 7, 8).

Results

After preparing the mud samples and following the procedure described above, extensive results were derived for density and rheology characteristics.

Density results

Below Table 2 presents the results obtained for the densities of all five mud samples in different units, as well as the temperature and pH of the samples.

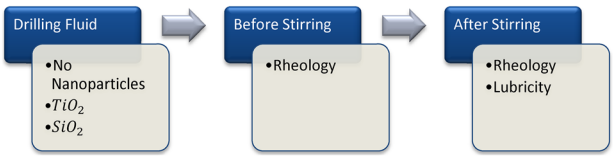

Fig. 8 Analysis performed after aging

Fig. 7 Aging cells and oven

Table 2 Densities of mud samples

Density						
Sample	PPG	SP GR	lb/ft^3	PSI/1000 ft	T (°C)	pH
Base mud	8.83	1.06	66.14	458.98	26	10
TiO_2 0.20%	8.83	1.06	66.14	458.98	26	10
TiO_2 0.60%	8.83	1.06	66.14	458.98	26	10
SiO_2 0.20%	8.85	1.062	66.27	459.85	26	10
SiO_2 0.60%	8.90	1.068	66.64	462.44	26	10

Table 3 Gel strength rheology of base mud (cP = centiPoise)

Rheology					
Base mud					
	Temp	Viscosity (cP)			
		Temperature			
		26 °C	40 °C	60 °C	80 °C
RPM (rad/s)	600	46.5	43	43.5	42
	300	33	31	31	30
	200	27	26	26	24.5
	100	20.5	20	19	17.5
	60	17	17	15.5	14.5
	30	14	13.5	13	11.5
	6	10	10	8.5	7.5
Gel strength (lb/100 ft^2)	10 s	9.5	9	7	7
	10 min	14	14	12	14.5

Rheology results

Before aging

The results of the RPM, viscosity and gel strength rheology obtained for each of the original and four nano-particle-doped mud samples (2 each for titania and silica nano-material) is detailed below, prior to aging. A graph of the shear stress vs the shear rate (RPM) for the different temperatures is also provided to show the trend of the mud samples.

Base mud: see Table 3 and Fig. 9.

Base mud with 0.20% (w/w) TiO_2: see Table 4 and Fig. 10.

Base mud with 0.60% (w/w) TiO_2: see Table 5 and Fig. 11.

Base mud with 0.20% (w/w) SiO_2: see Table 6 and Fig. 12.

Base mud with 0.60% (w/w) SiO_2: see Table 7 and Fig. 13.

After aging

After aging the mud samples for 16 h at 80 °C, the samples were cooled down to 26 °C. Following this, the rheological

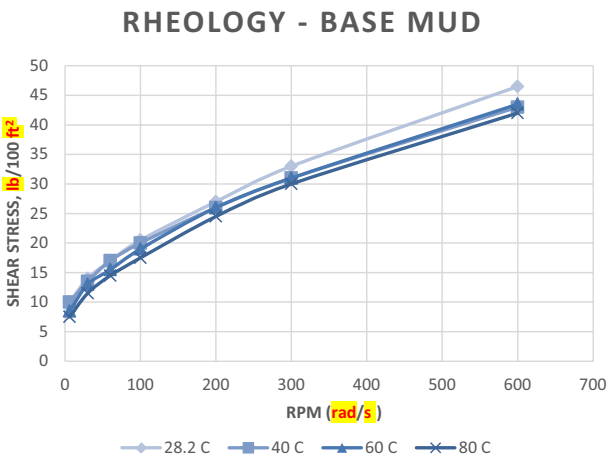

Fig. 9 Shear stress rheology of base mud (C = degrees Celsius)

Table 4 Gel strength rheology of base mud with 0.20% (w/w) TiO_2 (cP = centiPoise)

TiO_2 (0.20% w/w)					
		Viscosity (cP)			
		Temperature			
		26 °C	40 °C	60 °C	80 °C
RPM (rad/s)	600	50	49.5	47.5	51.5
	300	35.5	35	34	37
	200	29.5	29.5	28.5	31
	100	22.5	22.5	21.5	23
	60	19	19	18.5	19
	30	15.5	15.5	15	16
	6	10.5	10.5	10.5	11
Gel strength (lb/100 ft^2)	10 s	9.5	9.5	8.5	9.5
	10 min	14.5	14.5	14	16.5

experiments were re-conducted again at one temperature before and after stirring.

Before stirring See Table 8 and Fig. 14.

After stirring See Table 9 and Fig. 15.

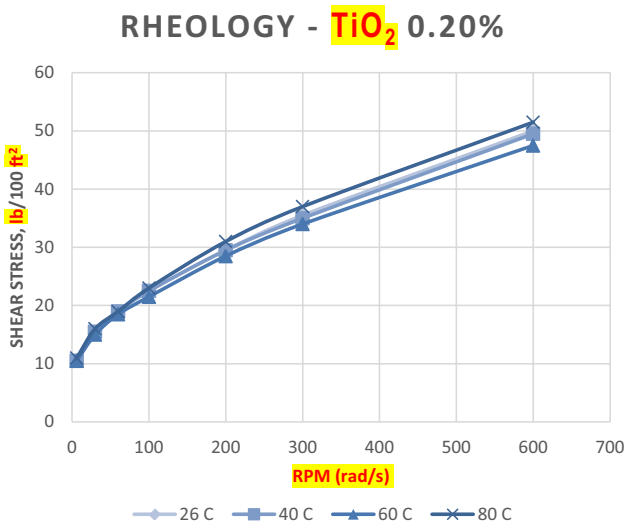

Fig. 10 Rheology of base mud with 0.20% (w/w) TiO_2 (C = degrees Celsius)

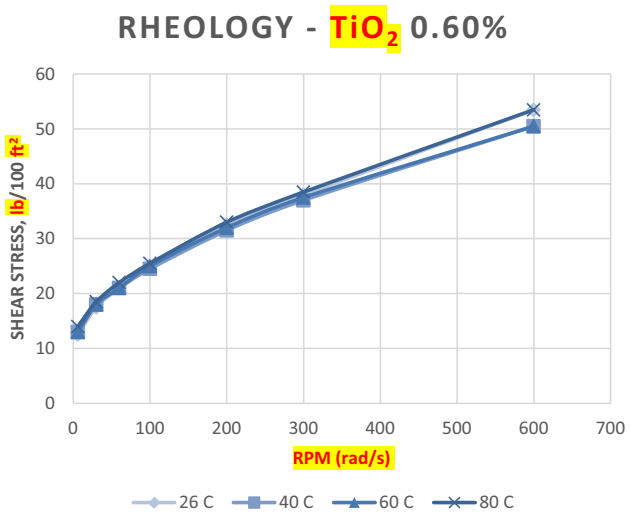

Fig. 11 Shear stress rheology of base mud with 0.60% (w/w) TiO_2 (C = degrees Celsius)

Table 5 Gel strength rheology of base mud with 0.60% (w/w) TiO_2 (cP = centiPoise)

Rheology					
TiO_2 (0.60% w/w)					
		Viscosity (cP)			
		Temperature			
		26 °C	40 °C	60 °C	80 °C
RPM (s^{-1})	600	53.5	50.5	50.5	53.5
	300	38	37	37.5	38.5
	200	32.5	31.5	32	33
	100	25	24.5	25	25.5
	60	21	21	21	22
	30	17.5	18	18	18.5
	6	12.5	13	13	14
Gel strength (lb/100 ft^2)	10 s	12	11	10	11.5
	10 min	16	16.5	16.5	19.5

Table 6 Gel strength rheology of base mud with 0.20% (w/w) SiO_2

Rheology					
SiO_2 (0.20% w/w)					
		Viscosity (cP)			
		Temperature			
		26 °C	40 °C	60 °C	80 °C
RPM (rad/s)	600	46	41	38.5	39.5
	300	31.5	29.5	28	27.5
	200	26.5	24.5	22.5	22
	100	19.5	18.5	16.5	15.5
	60	16	15.5	13	12
	30	12.5	12	10.5	9.5
	6	8	7.5	5.5	5.5
Gel strength (lb/100 ft^2)	10 s	8.5	8	6	6
	10 min	11.5	10.5	8.5	8

Lubricity results

Before evaluating the mud samples, the correction factor for the lubricity ring and lubricity block was calculated using Eq. (5). The result obtained is shown below:

$$\text{Correction factor} = \frac{34}{36} = 0.94. \quad (6)$$

Before aging

Similar to the rheology tests, the lubricity of the original and four nano-doped mud samples were evaluated at different temperatures as well. In this case, the data extracted is the *torque reading*. The following tables and graphs show the torque readings of the mud samples at different temperatures. The analysis of the lubricity is then subsequently conducted.

Base mud: see Table 10 and Fig. 16.

Base mud with 0.20% (w/w) TiO_2: see Table 11 and Fig. 17.

Base mud with 0.60% (w/w) TiO_2: see Table 12 and Fig. 18.

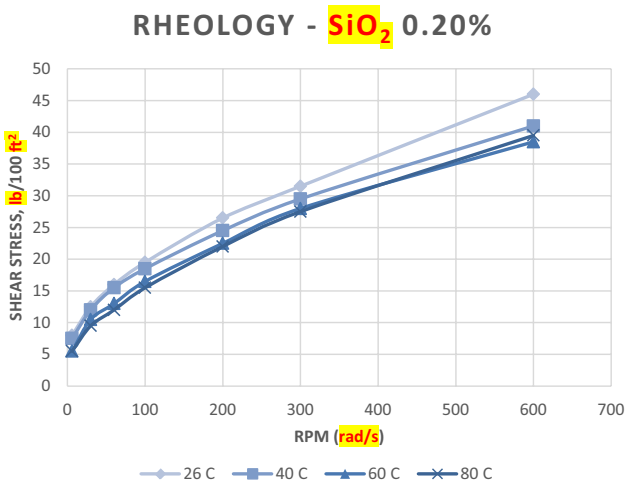

Fig. 12 Rheology of base mud with 0.20% (w/w) SiO_2 (C = degrees Celsius)

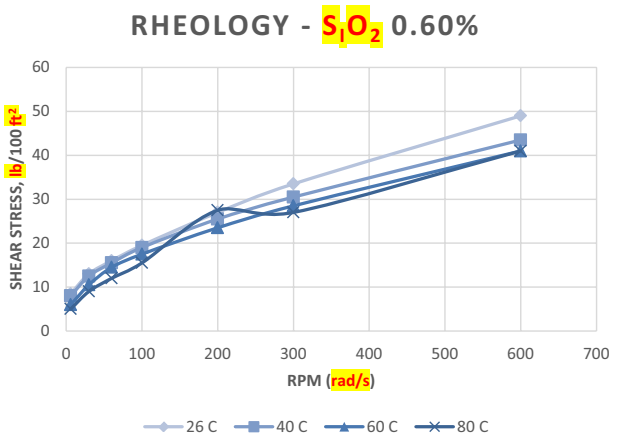

Fig. 13 Rheology of base mud with 0.60% (w/w) SiO_2 (C = degrees Celsius)

Table 7 Rheology of base mud with 0.60% (w/w) SiO_2

Rheology					
SiO_2 (0.60% w/w)					
		Viscosity (cP)			
		Temperature			
		26 °C	40 °C	60 °C	80 °C
RPM (rad/s)	600	49	43.5	41	41
	300	33.5	30.5	28.5	27
	200	27	25.5	23.5	27.5
	100	19.5	19	17.5	15.5
	60	16	15.5	14.5	12
	30	13	12.5	10.5	9
	6	8.5	8	6	5
Gel strength (lb/100 ft^2)	10 s	9	8	7	6
	10 min	11	10	9	7.5

Base mud with 0.20% (w/w) SiO_2: see Table 13 and Fig. 19.
Base mud with 0.60% (w/w) SiO_2: see Table 14 and Fig. 20.

After aging

The lubricity test was repeated for all five mud samples after the aging process and stirring them in the mixer for 10 min. The results are shown below (Table 15; Fig. 21).

Analysis and discussion

In this section, we interpret the results presented earlier. Each set of results pertaining to different aspects of the investigation is addressed individually i.e., density, rheology and lubricity. The density unit used is that consistent with modern petroleum engineering, namely lbm/gal (also known as ppg i.e., pounds per gallon).

Density

Inspection of Table 2 reveals that density of the mud samples was very similar after the addition of nano-particles. There was only a small increase when silica nano-particles were added, while the variation in concentration of titania nano-particles did not show any tangible alteration. This increment observed with silica nano-particles was proportional to the concentration of these nano-particles in the base mud, and this has been calculated and listed in Table 16. These results suggest that silica nano-particles could have acted as weighting agents which could be applicable in actual water-based mud suspensions in the field where even a slight modification in density may be beneficial to drilling (Mostafavi et al. 2011).

Rheology-before aging

In general, the results of the rheology tests (before aging) of the mud samples doped with nano-particles, which are plotted from Figs. 10, 11, 12, 13, 14 and 15 demonstrate the normal trend of typical drilling muds i.e., without nano-particles (sample 1, Fig. 9). The analysis of the rheological properties was done using the Bingham (viscoplastic) model and the curves of each mud sample were adapted to this model. However, this model is not representative of the drilling mud behaviour at low shear rates. The plastic viscosity, yield point and apparent viscosity were calculated using Eqs. (1)–(3), respectively. An example of the calculation of these parameters for the base mud at 26 °C follows:

Plastic viscosity:

Table 8 Rheology of aged mud samples before stirring

Rheology						
After aging—before stirring						
		Viscosity (cP)				
		Mud sample				
		Base mud	TiO_2 0.20%	TiO_2 0.60%	SiO_2 0.20%	SiO_2 0.60%
RPM (rad/s)	600	39	50	44	54	63.5
	300	26.5	35	30.5	38	44.5
	200	21	28	24.5	30.5	35.5
	100	14	20	17.5	21	25.5
	60	11	16	14	17.5	19.5
	30	8.5	12	10.5	12.5	14.5
	6	5	7	7	6.5	8
Gel strength (lb/100 ft^2)	10 s	5	6.5	7	6	8
	10 min	7	9.5	9	7.5	9

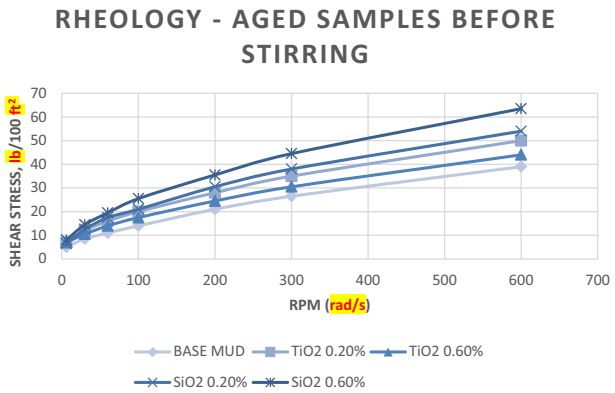

Fig. 14 Rheology of aged mud samples before stirring

$$\mathrm{PV}_{\text{Base Mud (26 °C)}} = 600\,\text{RPM reading} - 300\,\text{RPM reading} = 46.5 - 33 = 13.5\,\text{cp}. \quad (7)$$

Yield point:

$$\mathrm{YP}_{\text{Base Mud (26 °C)}} = 300\,\text{RPM reading} - \mathrm{PV} = 33 - 13.5 = 19.5\,\text{lb}/100\,\text{ft}^2. \quad (8)$$

Apparent viscosity:

$$\mathrm{AV}_{\text{Base Mud (26 °C)}} = \frac{600\,\text{RPM reading}}{2} = \frac{46.5}{2} = 23.25\,\text{cp}. \quad (9)$$

The same procedure was repeated for the other results obtained in Tables 3, 4, 5, 6, 7, 8 and 9.

Table 9 Rheology of aged mud samples after stirring

Rheology						
After aging—after stirring						
		Viscosity (cP)				
		Mud sample				
		Base mud	TiO_2 0.20%	TiO_2 0.60%	SiO_2 0.20%	SiO_2 0.60%
RPM (rad/s)	600	26.5	34.5	32	33	38.5
	300	18	24	22	22	26
	200	15	19.5	18	18.5	20.5
	100	10.5	13.5	13	12	14.5
	60	7.5	11	10	8.5	11
	30	5.5	8	7.5	6	8
	6	3	4.5	4	3.5	4.5
Gel strength (lb/100 ft^2)	10 s	4	4.5	5	4.5	5
	10 min	7	7	8	6	7

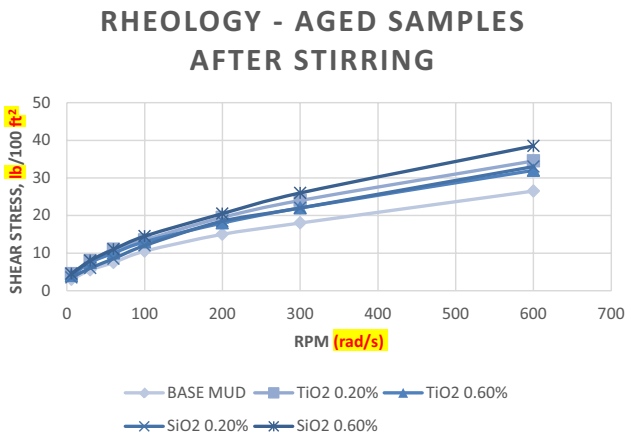

Fig. 15 Rheology of aged mud samples after stirring

Table 10 Torque readings of base mud

Lubricity test					
Base mud					
		Temperature			
	Time (min)	26 °C	40 °C	60 °C	80 °C
Torque reading (in.-pounds)	1	37.5	42.3	45.2	43.6
	2	39.5	42.4	44.4	44.4
	3	40	42	44.4	45.5
	4	40	41.4	44.6	45.8
	5	39.9	40.7	44.6	46.1
	6	39.6	41.1	45	46.6

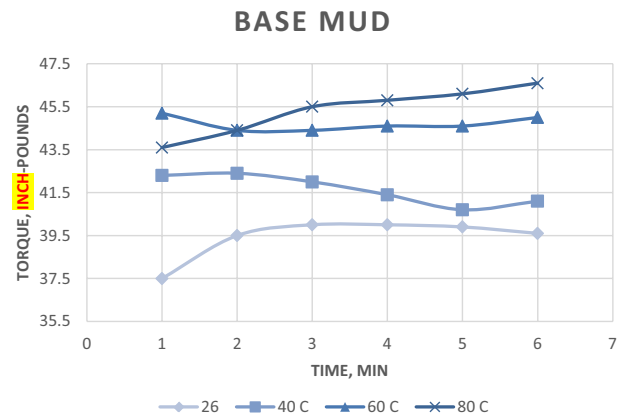

Fig. 16 Torque readings of base mud (C = degrees Celsius)

Table 17 summarizes these calculations using the Bingham model (a yield stress is required to initiate flow), and presents the increase (green arrow) and decrease (red arrow) of these parameters compared to the base mud (yellow dash) for each temperature. The evaluation of the

Table 11 Torque readings of base mud with 0.20% (w/w) TiO_2

Lubricity test					
TiO_2 (0.20% w/w)					
		Temperature			
	Time (min)	26 °C	40 °C	60 °C	80 °C
Torque reading (in.-pounds)	1	42.4	42.7	47.9	44.4
	2	44.5	43.3	48.5	44.6
	3	44.2	44.1	48.6	44.4
	4	44.6	45.2	48.4	46.3
	5	45.9	46	47.7	45.7
	6	46.1	45.3	47	45.6

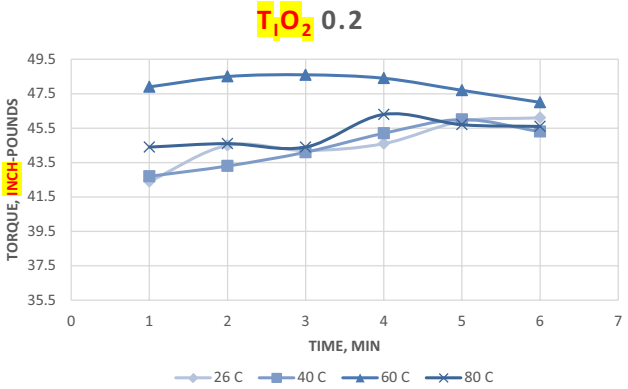

Fig. 17 Torque readings of base mud with 0.20% (w/w) TiO_2 (C = degrees Celsius)

Table 12 Torque readings of base mud with 0.60% (w/w) TiO_2

Lubricity test					
TiO_2 (0.60% w/w)					
		Temperature			
	Time (min)	26 °C	40 °C	60 °C	80 °C
Torque reading (in.-pounds)	1	40.2	39.2	39.3	39
	2	40	37.7	38.4	39.4
	3	40	37.4	37.9	39.3
	4	39.3	36.7	37.6	39.4
	5	38.7	35.9	37.6	39
	6	37.9	36.2	37.4	39.6

rheology at different temperatures showed that the viscosity readings were different for each case, although, they were close to the base mud results. From Figs. 9, 10, 11, 12 and 13, it is evident that titania nano-particles provided higher viscosity than base mud or silica-doped mud. Silica nano-particles in fact reduced the viscosity of the mud. In general, the viscosity of all the mud samples tended to

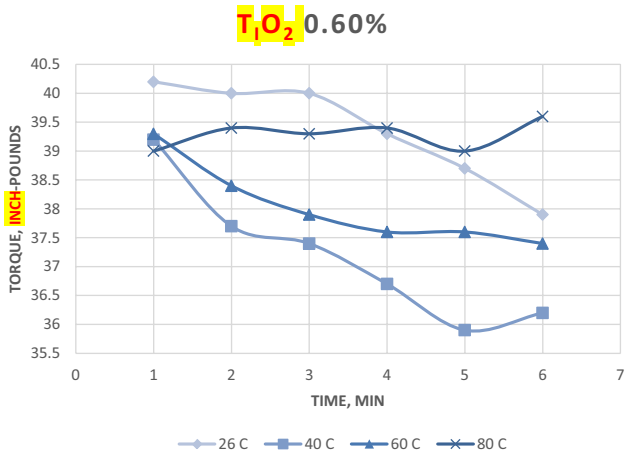

Fig. 18 Torque readings of base mud with 0.60% (w/w) TiO_2 (C = degrees Celsius)

Table 13 Torque readings of base mud with 0.20% (w/w) SiO_2

Lubricity test					
SiO_2 (0.20% w/w)					
		Temperature			
	Time (min)	26 °C	40 °C	60 °C	80 °C
Torque reading (in.-pounds)	1	37	40.6	42.5	43.9
	2	38.8	41.2	42.7	44.5
	3	39.1	42.3	43.3	44.1
	4	39.8	42.5	43.9	44.7
	5	40.7	42.8	43.6	44.7
	6	40.2	43.1	43.4	44.2

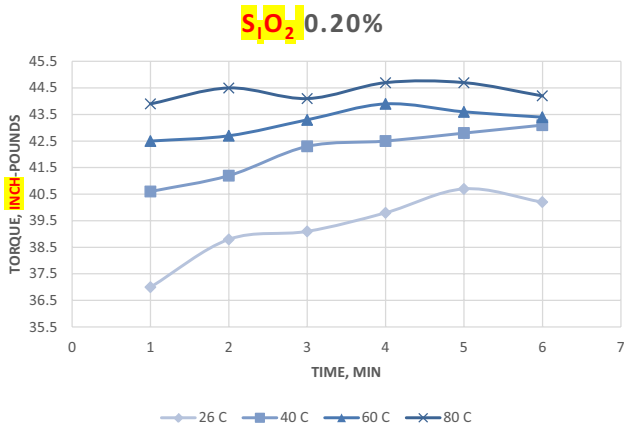

Fig. 19 Torque readings of base mud with 0.20% (w/w) SiO_2 (C = degrees Celsius)

increase at high shear rates. Moreover, in the case of silica nano-particles and base mud, the viscosity was reduced when the temperature was increased. However, in the case

Table 14 Torque readings of base mud with 0.60% (w/w) SiO_2

Lubricity test					
SiO_2 (0.60% w/w)					
		Temperature			
	Time (min)	26 °C	40 °C	60 °C	80 °C
Torque reading (in.-pounds)	1	47	43.2	43.9	44.8
	2	46.2	41.6	44.7	44.4
	3	45.2	41	44	43.7
	4	43.8	40.6	43.7	43.5
	5	42.6	40	43.2	43.1
	6	43.4	40.4	43.1	42.8

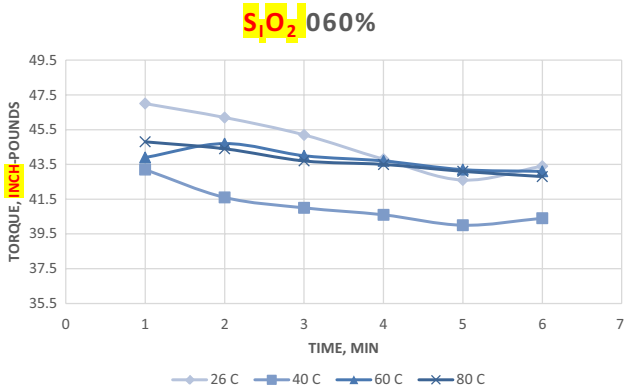

Fig. 20 Torque readings of base mud with 0.60% (w/w) SiO_2 (C = degrees Celsius)

of titania nano-particles, it is apparent that the variations of viscosity at different shear rates remained almost the same for all the temperatures. A possible explanation for this behaviour is that silica nano-particles are hydrophilic, so that the amount of solid particles in the base mud is in fact drastically reduced and they do not improve, therefore, the viscosity of the base mud as titania nano-particles. It is also important to note that in general, titania nano-particles showed an increase in plastic viscosity (PV), yield point (YP) and apparent viscosity (AV), although they exhibit a decrease in yield point when the concentration is lower i.e., 0.20% (w/w) at 40 °C. The addition of silica nano-particles results in a decrease in the yield point, and a similar trend in apparent viscosity although there is a deviation from this at a concentration of 0.60% (w/w), where viscosity increases at 26 and 40 °C. Some fluctuation in results is also evident with temperature and a consistent trend is not attained for plastic viscosity with silica. Plastic viscosity tends to increase in drilling fluids due to an excess in the number of particles, which in turn causes an increase in the mechanical friction between solids and liquids in the mud system (Hughes 1995). Taking

Table 15 Torque readings of aged mud samples after stirring

Lubricity test						
After aging—after stirring						
		Mud samples				
	Time (min)	Base mud	TiO_2 0.20%	TiO_2 0.60%	SiO_2 0.20%	SiO_2 0.60%
Torque reading	1	28	36.5	33.1	40.4	37.5
	2	32.9	35.8	33.6	38.8	38.4
	3	34.1	36.8	33.6	37.8	38
	4	34.8	36.1	33.8	37.1	38.4
	5	34.3	36	33.7	37.3	38.4
	6	34.1	35.9	33.9	36.9	38

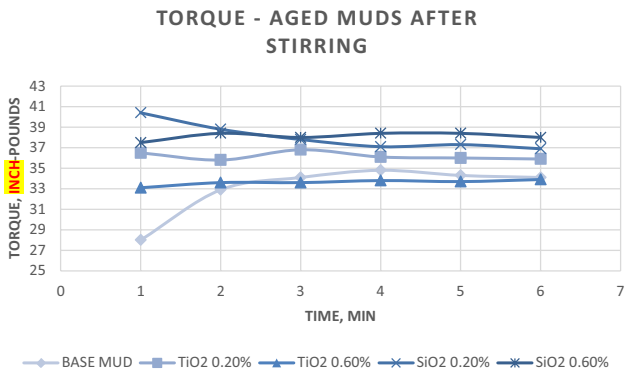

Fig. 21 Torque readings of aged mud samples after stirring

Table 16 Variation in density with nano-particles

DENSITY		
SAMPLE	PPG	INCREASE (%)
BASE MUD	8.83	-
TiO2 0.20 %	8.83	0
TiO2 0.60 %	8.83	0
SiO2 0.20 %	8.85	0.23
SiO2 0.60 %	8.90	0.79

into account this antecedent and the concentrations used for each nanoparticle, 0.20% (w/w) and 0.60% (w/w), and assuming that the morphology of both nano-particles was spherical the number of titania particles per 350 ml was roughly 1.17×10^{16} and 3.51×10^{16}, respectively. However, the number of silica particles for the same amount of liquid was about 6.33×10^{16} and 19.01×10^{16} which is significantly larger and may be counter-productive for mud rheology. Furthermore, the calculation is not exact since the structure of both nano-particles are not *exactly spherical*, as described in the property tables given in the Appendix, but approximations. A visualization of the variation of plastic viscosity for all five samples is given in Fig. 22.

In the case of silica nano-particles, the super hydrophilic characteristic (due to their coating agent) may have reduced the amount of solid silica nano-particles dispersed in the drilling mud. The plastic viscosity achieved when titania was added almost invariant with different temperatures and did not follow the normal decreasing trend of the base mud. A normal mud tends to decrease in plastic viscosity when its temperature is raised since the viscosity of the water decreases (Hughes 1995). This effect may furthermore contribute to improved thermal conductivity of titania nano-particles in the base mud. Regarding the yield point, this parameter is an indicator of the chemical attraction of the particles in the drilling mud. When the balance is broken, the yield point tends to increase. This may arise due to the addition of inert solids and the volume concentration of solids although many other micro-structural features may also contribute. In the case of titania nano-particles, these nano-particles may not have interacted with the rest of the additives, acting as inert particles, in the drilling mud which may manifest in an increase in yield point. In the case of silica nano-particles, the super hydrophilic feature could have caused a reduction in yield point since these particles were probably dissolved in the drilling mud, which is water based, which results in a decrease in volume concentration of solids. Therefore, the addition of titania nano-particles in the base mud indicates that this nano-particle-doped mud sample requires greater shear stress to initiate motion of the drilling mud, as shown in Fig. 23. Conversely, the addition of silica nano-particles requires less stress for mobilizing flow of the drilling mud. Although lower yield stress may have advantages, it can also lead to problems in the reduced ability of the drilling mud to suspend drill cuttings when drilling.

The relationship between both parameters (YP/PV), yield point and plastic viscosity, is useful to determine the *efficiency of the drilling mud* when cleaning the well. A low plastic viscosity and a high yield point give an optimum efficiency. The results in Fig. 24 show that titania nano-particles achieve the highest increase in this relationship, which is proportional to the increase in

Table 17 Results of PV, YP, YP/PV and AV of mud samples before aging

RHEOLOGY					
PV - YP - AV					
BEFORE AGING					
T (°C)	SAMPLE	PV (CP)	YP (lb/100 ft2)	YP/PV	AV (cp)
26	**BASE MUD**	**13.5**	**19.5**	**1.44**	**23.25**
	TiO2 0.20%	14.5	21	1.45	25
	TiO2 0.60%	15.5	22.5	1.45	26.75
	SiO2 0.20%	14.5	17	1.17	23
	SiO2 0.60%	15.5	18	1.16	24.5
40	**BASE MUD**	**12**	**19**	**1.58**	**21.5**
	TiO2 0.20%	14.5	10.5	0.43	29.75
	TiO2 0.60%	13.5	23.5	1.74	25.25
	SiO2 0.20%	11.5	18	1.57	20.5
	SiO2 0.60%	13	17.5	1.35	21.75
60	**BASE MUD**	**12.5**	**18.5**	**1.48**	**21.75**
	TiO2 0.20%	13.5	20.5	1.52	23.75
	TiO2 0.60%	13	24.5	1.88	25.25
	SiO2 0.20%	10.5	17.5	1.67	19.25
	SiO2 0.60%	12.5	16	1.28	20.5
80	**BASE MUD**	**12**	**18**	**1.50**	**21**
	TiO2 0.20%	14.5	22.5	1.55	25.75
	TiO2 0.60%	15	23.5	1.57	26.75
	SiO2 0.20%	12	15.5	1.29	19.75
	SiO2 0.60%	14	13	0.93	20.5

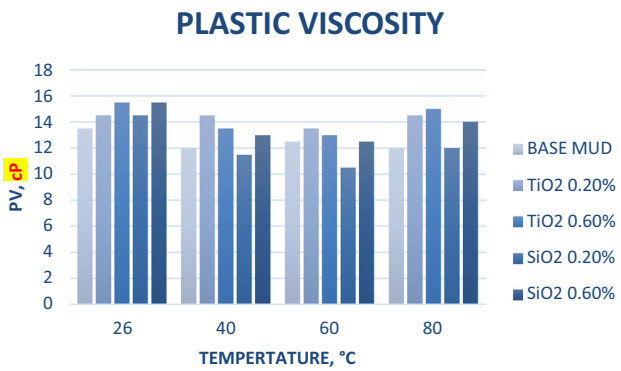

Fig. 22 Plastic viscosity before aging

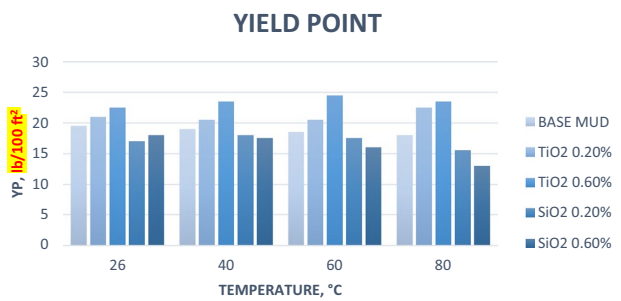

Fig. 23 Yield point before aging

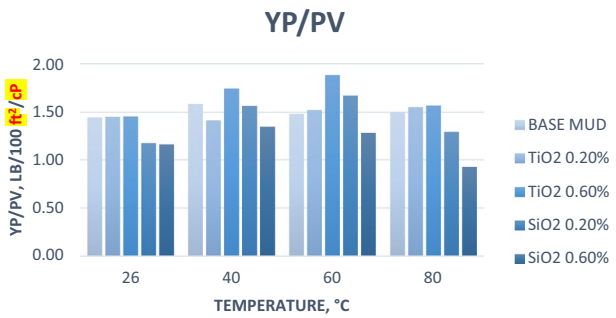

Fig. 24 YP/PV relationship before aging

concentration and is slightly greater than the base mud. On the other hand, silica nano-particles showed the lowest efficiency and an inversely proportional relationship with the increase in concentration. Therefore, the addition of silica nano-particles could cause problems related to the cleaning efficiency of the drilling mud, whereas titania nano-particles could contribute to improving it.

In the case of apparent viscosity (Fig. 25), titania nano-particles had the highest values, while silica nano-particles had the lowest. Although, this parameter does not give an exact indication of the real viscosity, it is useful to diagnose problems when drilling. It was calculated in the present study by dividing the viscosity reading at 600 RPM by two, so that from the column chart below, it is noticed that

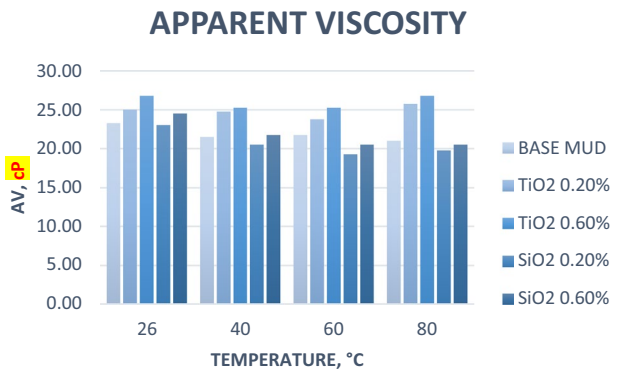

Fig. 25 Apparent viscosity before aging

the titania nano-particles showed the *highest viscosities* at *high shear rate* (Table 18).

In the case of gel strength, the greatest increase at different temperatures was mostly in the base mud, obtaining 85.71% at 80 °C, as it is plotted in Fig. 26. However, the readings at 10 s and 10 min for both concentrations of titania nano-particles were the largest in magnitude. Silica nano-particles demonstrated the *lowest values* in both cases. These results indicate that addition of titania in the base mud tends to create *a gel structure* quicker than the base mud over time. Moreover, this effect was more prominent when the concentration was increased. This may, however, be beneficial in slowing down the settlement of drill cuttings when mud circulation is stopped in highly deviated wells.

Silica nano-particles also showed an increase over time in gel strength parameter when the concentration was increased, although it was minor compared to the other mud samples. In addition, these results indicate that silica nano-particles could reduce the performance of the drilling mud and induce operational problems, including mechanical sticking of the drill string due to a possible accumulation of drill cuttings. However, silica nano-particles could prove beneficial in that they could be introduced into the drilling mud to reduce the gel strength of the drilling fluid when it is too high. Regarding gel strength classification, there was insufficient data over time to determine if any of the mud samples showed a progressive or regressive trend. However, it is noteworthy that there is a reduction in the percentage of the gel strength increase when the concentration of nano-particles is raised. This could indicate that a higher concentration of these nano-particles produces a slow increment of

Table 18 Summarizes the analysis for the rheological gel strength in the drilling mud samples and results of the increase in gel strength of mud samples before aging

RHEOLOGY				
GEL STRENGTH				
BEFORE AGING				
T (°C)	SAMPLE	10 sec	10 min	INCREASE (%)
26	**BASE MUD**	**9.5**	**14**	**47.37**
	TiO2 0.20%	9.5	14.5	52.63
	TiO2 0.60%	12	16	33.33
	SiO2 0.20%	8.5	11.5	35.29
	SiO2 0.60%	9	11	22.22
40	**BASE MUD**	**9**	**14**	**55.56**
	TiO2 0.20%	9.5	14.5	52.63
	TiO2 0.60%	11	16.5	50.00
	SiO2 0.20%	8	10.5	31.25
	SiO2 0.60%	8	10	25.00
60	**BASE MUD**	**7**	**12**	**71.43**
	TiO2 0.20%	8.5	14	64.71
	TiO2 0.60%	10	16.5	65.00
	SiO2 0.20%	6	8.5	41.67
	SiO2 0.60%	7	9	28.57
80	**BASE MUD**	**7**	**13**	**85.71**
	TiO2 0.20%	9.5	16.5	73.68
	TiO2 0.60%	11.5	19.5	69.57
	SiO2 0.20%	6	8	33.33
	SiO2 0.60%	6	7.5	25.00

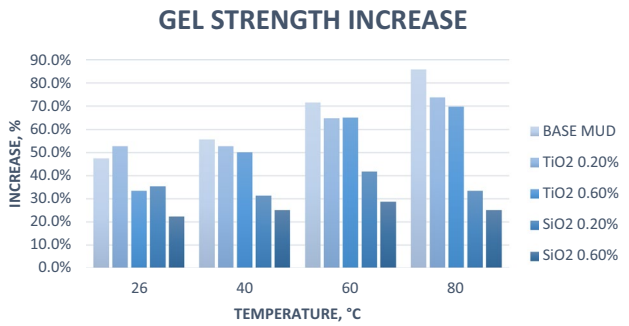

Fig. 26 Gel strength increase over time before aging

the gel strength over time. Furthermore, the increase of gel strength on the base mud and titania nano-particles could be due to a reduction in the water viscosity generated by an increase in temperature, which is also relevant to higher temperature-drilling operations (Gray et al. 1980).

Rheology after aging

In the post-aging case, the rheology was tested before stirring the mud samples in the mixer and after stirring them. The intention of testing the mud samples before stirring them was to simulate how they could behave once the drill string start to rotate again, after being static for a period. The evaluation after stirring them was done to simulate their behaviour *after the drilling mud have been circulated for a period*. Two sets of results were, therefore, obtained.

Before stirring

Making a comparison between Figs. 14 and 15, there is a tangible elevation in the viscosity for both concentrations of silica nano-particles *after the aging process* before stirring the mud sample. These readings were higher than the mud sample with titania nano-particles and the base mud. In the case of the mud sample with titania nano-particles and the base mud, the viscosities decreased after the aging process. This may be attributable to degradation of the other additives (viscosifier agent) in the base mud. The highest increase in plastic viscosity, yield point and apparent viscosity was for silica nano-particles; in addition, these results were also higher than the readings at the same temperature before aging. This could indicate that after the aging process, flocculation took place and the mechanical friction between particles increased in the drilling mud with silica nano-particles.

The results for the base mud in Table 19 indicate a decreasing trend in their rheological properties. In the case of yield point, the values indicate that these mud samples may struggle to perform some of their functions, such as carrying drill cuttings, after being static for a long time. A similar deduction may apply to the drilling mud with titania nano-particles which also exhibit a decreasing trend in yield point. Moreover, the reduction in plastic viscosity of the base mud could be due to a reduction in the mechanical friction of the embedded nano-particles.

In the case of gel strength, all the results showed a poor performance, as can be observed in Table 20. It is also apparent, however, that the increase in gel strength in silica nano-particles compared to the base mud, was lower before the aging process. However, due to the low results in gel strength, it would appear that the mud samples are not able to suspend drill cuttings after being static at borehole conditions over a long period which could cause operational issues.

Table 20 Results of gel strength of mud samples after aging before stirring

RHEOLOGY				
GEL STRENGTH				
AFTER AGING - BEFORE STIRRING				
T (°C)	SAMPLE	10 sec	10 min	INCREASE (%)
26	BASE MUD	5	7	40%
	TiO2 0.20%	6.5	9.5	46%
	TiO2 0.60%	7	9	29%
	SiO2 0.20%	6	7.5	25%
	SiO2 0.60%	8	9	13%

Table 19 Results of PV, YP, YP/PV and AV of mud samples after aging before stirring

RHEOLOGY					
PV - YP - YP/PV					
AFTER AGING - BEFORE STIRRING					
T (°C)	SAMPLE	PV (CP)	YP (lb/100 ft2)	YP/PV	AV (cp)
26	BASE MUD	12.5	14	1.12	19.5
	TiO2 0.20%	15	20	1.33	25
	TiO2 0.60%	13.5	17	1.26	22
	SiO2 0.20%	16	22	1.38	27
	SiO2 0.60%	19	25.5	1.34	31.75

Table 21 Results of PV, YP, YP/PV and AV of mud samples after aging after stirring

RHEOLOGY					
PV - YP - AV					
AFTER AGING - AFTER STIRRING					
T (°C)	SAMPLE	PV (CP)	YP (lb/100 ft2)	YP/PV	AV (cp)
26	BASE MUD	8.5	9.5	1.12	13.25
	TiO2 0.20%	10.5	13.5	1.29	17.25
	TiO2 0.60%	10	12	1.20	16
	SiO2 0.20%	11	11	1.00	16.5
	SiO2 0.60%	12.5	13.5	1.08	19.25

After stirring

After stirring the mud samples, it can be observed at Fig. 15 that the viscosity readings during different shear rates decreased further, for all the mud samples. However, a similar trend to the previous case is observed; the highest viscosity readings were obtained with 0.60% (w/w) SiO_2, and the lowest were for the base mud without any nano-particles.

Tables 21 and 22 shows that there were not a favorable trend on rheological properties of the drilling mud samples after stirring them in the mixer. In fact, all the results were lower than the rheological tests before stirring. This loss in viscosity may be directly attributable to the degradation of the viscosifier agent during the aging process.

Lubricity

The results obtained during the lubricity test indicated that titania nano-particles at a concentration of 0.60% (w/w) gave the best performance for torque compared to the other mud samples, although, a large decrease in torque was not observed. However, taking into account that the torque readings in the base mud tended to increase over time before and after aging, these results could be relevant. To evaluate the lubricity of the mud samples, the CoF was calculated using Eq. (4). This factor provides a more accurate value for the trend of the lubricity during the tests since it incorporates a correction factor. For the case of the base mud, the CoF for the base mud is calculated as follows:

$$\mathrm{CoF}_{\text{Base Mud (26 °C,1 min)}} = \frac{37.5\ \text{in.-pounds} \times 0.94}{100\ \text{lbf}} \tag{10}$$

$$\mathrm{CoF}_{\text{Base Mud (26 °C,1 min)}} = 0.35. \tag{11}$$

The same calculation was performed for the rest of the mud samples. We consider again both cases before aging and after aging.

Table 22 Results of gel strength of mud samples after aging after stirring

RHEOLOGY				
GEL STRENGTH				
AFTER AGING - AFTER STIRRING				
T (°C)	SAMPLE	10 sec	10 min	INCREASE (%)
26	BASE MUD	4	7	75%
	TiO2 0.20%	4.5	7	56%
	TiO2 0.60%	5	8	60%
	SiO2 0.20%	4.5	6	33%
	SiO2 0.60%	5	7	40%

Before aging

From the results of the lubricity test, which can be observed from Tables 10, 11, 12, 13 and 14 and from Figs. 16, 17, 18, 19 and 20, it can be appreciated that the results of titania nano-particles at a concentration of 0.60% (w/w) showed a decreasing trend (and the lowest values) for the torque readings at different temperatures. However, at a lower concentration (0.20% w/w), they showed the highest torque readings. In the case of silica nano-particles, at a concentration of 0.20% (w/w), the torque readings were close to the base mud and showed a stable growth over time. However, when their concentration was raised, the torque also increased; however, these readings decreased over time, although, they were not lower than the results of the base mud. Table 23 shows the variation in percentage of the torque readings of the treated base mud with nano-particles relative to the untreated base mud. Here (and also in Table 24), a negative value means a reduction and a positive value means an increase, moreover, the results are highlighted with a blue colour scale which gets darker with an increase in the percentage.

In Table 23, the highest decrease in percentage was for titania nano-particles at 0.60% (w/w) and the torque percentage tended to reduce with an increase in temperature, as well as, silica nano-particles at 0.60% (w/w). Moreover, titania nano-particles at 0.20% (w/w) and silica nano-particles at 0.20% (w/w), both showed a decreasing trend from 60 °C,

Table 23 Percentage in torque variation before aging

TORQUE VARIATION (%) BEFORE AGING								
		TIME (MIN)						
SAMPLE	TEMP (°C)	1	2	3	4	5	6	SPARKLINES
TiO2 0.20%	26	13.1%	12.7%	10.5%	11.5%	15.0%	16.4%	
	40	0.9%	2.1%	5.0%	9.2%	13.0%	10.2%	
	60	6.0%	9.2%	9.5%	8.5%	7.0%	4.4%	
	80	1.8%	0.5%	-2.4%	1.1%	-0.9%	-2.1%	
TiO2 0.60%	26	7.2%	1.3%	0.0%	-1.8%	-3.0%	-4.3%	
	40	-7.3%	-11.1%	-11.0%	-11.4%	-11.8%	-11.9%	
	60	-13.1%	-13.5%	-14.6%	-15.7%	-15.7%	-16.9%	
	80	-10.6%	-11.3%	-13.6%	-14.0%	-15.4%	-15.0%	
SiO2 0.20%	26	-1.3%	-1.8%	-2.3%	-0.5%	2.0%	1.5%	
	40	-4.0%	-2.8%	0.7%	2.7%	5.2%	4.9%	
	60	-6.0%	-3.8%	-2.5%	-1.6%	-2.2%	-3.6%	
	80	0.7%	0.2%	-3.1%	-2.4%	-3.0%	-5.2%	
SiO2 0.60%	26	25.3%	17.0%	13.0%	9.5%	6.8%	9.6%	
	40	2.1%	-1.9%	-2.4%	-1.9%	-1.7%	-1.7%	
	60	-2.9%	0.7%	-0.9%	-2.0%	-3.1%	-4.2%	
	80	2.8%	0.0%	-4.0%	-5.0%	-6.5%	-8.2%	

Table 24 Coefficient of friction before aging

COF BEFORE AGING									
		TIME							
SAMPLE	TEMP (°C)	1	2	3	4	5	6	SPARKLINES	AVERAGE
BASE MUD	26	0.354	0.373	0.378	0.378	0.377	0.374		0.37
	40	0.399	0.400	0.396	0.391	0.384	0.388		0.39
	60	0.427	0.419	0.419	0.421	0.421	0.425		0.42
	80	0.412	0.419	0.430	0.432	0.435	0.440		0.43
TiO2 0.20%	26	0.400	0.420	0.417	0.421	0.433	0.435		0.42
	40	0.403	0.409	0.416	0.427	0.434	0.428		0.42
	60	0.452	0.458	0.459	0.457	0.450	0.444		0.45
	80	0.419	0.421	0.419	0.437	0.431	0.430		0.43
TiO2 0.60%	26	0.379	0.378	0.378	0.371	0.365	0.358		0.37
	40	0.370	0.356	0.353	0.346	0.339	0.342		0.35
	60	0.371	0.362	0.358	0.355	0.355	0.353		0.36
	80	0.368	0.372	0.371	0.372	0.368	0.374		0.37
SiO2 0.20%	26	0.349	0.366	0.369	0.376	0.384	0.379		0.37
	40	0.383	0.389	0.399	0.401	0.404	0.407		0.40
	60	0.401	0.403	0.409	0.414	0.412	0.410		0.41
	80	0.414	0.420	0.416	0.422	0.422	0.417		0.42
SiO2 0.60%	26	0.444	0.436	0.427	0.413	0.402	0.410		0.42
	40	0.408	0.393	0.387	0.383	0.378	0.381		0.39
	60	0.414	0.422	0.415	0.413	0.408	0.407		0.41
	80	0.423	0.419	0.413	0.411	0.407	0.404		0.41

although both of them show some fluctuation. Regarding the CoF analysis, Table 24 shows the results for the torque readings at different temperatures using the same format as Table 23.

A similar trend for the mud samples with nano-particles is evident as in the case of Table 23. Moreover, an increasing trend in the CoF of the base mud with a rise of temperature is clearly evident in Table 24. These tables imply that the addition of silica nano-particles in the base mud tends to improve the lubricity, even with a small concentration. In addition, these trends suggest that it could be necessary to increase the nano-particle concentration to achieve better results, since the maximum reduction in torque was about 8%. However, in the case of titania nano-particles the highest reduction in torque was about 16% (double that of silica nano-particles). The reduction in torque and CoF of titania nano-particles at 0.60% (w/w) would also suggest that an increase in their concentration could further depress both parameters, with the implication that titania nano-particles could have a greater impact in the improvement of drilling mud lubricity than silica nano-particles. Lubricity refers to the reduction in friction and or wear by a lubricant and, therefore, the presence of titania nano-particles offers clear tribological advantages. The Tables 23 and 24 further show that the torque and CoF of the base mud increases with temperature, whereas the addition of nano-particles in the base mud shows the contrary effect. The reduction is more significant with a higher concentration of titania nano-particles and this may also be an evidence for the improved thermal conductivity (and therefore heat dissipation characteristic) of nano-particles, which has been emphasized in numerous experimental studies including (Choi 1995; Hung and Gu 2014) Due to the presence of nano-particles around the lubricating film created between the lubricity ring and block in the lubricity tests, the nano-particles may have isolated and dissipated the heat more efficiently around this film. Silica and titania are both ceramic materials which are known to have excellent thermal dissipation properties. As nano-particles these materials retain this feature.

After aging

In this case, the lubricity test was carried out *only after stirring* the mud samples and cooling them to recreate the lubricity behaviour representative of drilling muds after circulation for some time after following a period in which they are static at the bottom hole condition. From Table 15 and Fig. 21 ("Results") it can be observed that the results were lower than the previous test at the same temperature (before the aging process), although, the growing trend exhibited by the base mud remained. However, the other mud samples did not exhibit the same pattern. For titania and silica nano-particles at 0.60% (w/w), the trend changed and remained stable with slight fluctuations, while titania and silica at 0.20% (w/w) showed a decreasing trend. Below, Table 25 shows the torque variation in percentage after the aging process compared to the base mud.

In this scenario, the torque variation for all the mud samples with nano-particles showed a considerable drop after the first minute of the test, and then, it was followed by a moderate fall over time. However, in most samples, the reduction was not below than the torque readings of the base

Table 25 Percentage in torque variation after aging

TORQUE VARIATION (%) AFTER AGING								
		TIME (MIN)						
TEMP (°C)	SAMPLE	1	2	3	4	5	6	SPARKLINES
26	TiO2 0.20%	30.4%	8.8%	7.9%	3.7%	5.0%	5.3%	
	TiO2 0.60%	18.2%	2.1%	-1.5%	-2.9%	-1.7%	-0.6%	
	SiO2 0.20%	44.3%	17.9%	10.9%	6.6%	8.7%	8.2%	
	SiO2 0.60%	33.9%	16.7%	11.4%	10.3%	12.0%	11.4%	

Table 26 Coefficient of friction after aging

COF AFTER AGING									
		TIME (MIN)							
TEMP (°C)	SAMPLE	1	2	3	4	5	6	SPARKLINES	AVERAGE
26	BASE MUD	0.263	0.309	0.321	0.327	0.322	0.321		0.311
	TiO2 0.20%	0.343	0.337	0.346	0.339	0.338	0.337		0.340
	TiO2 0.60%	0.311	0.316	0.316	0.318	0.317	0.319		0.316
	SiO2 0.20%	0.380	0.365	0.355	0.349	0.351	0.347		0.358
	SiO2 0.60%	0.353	0.361	0.357	0.361	0.361	0.357		0.358

mud; only titania nano-particles at 0.60% (w/w) were below the base mud values. Finally, Table 26 shows the results of the calculation of the CoF after aging. In general, the results follow the same trend as the torque readings of this test. The friction factors of the mud with nano-particles were close to the base mud friction factor.

In general, the results of the lubricity after the aging process demonstrated the best performance for all the mud samples. All of these results showed a considerable reduction in the CoF compared to the results before aging. However, only titania nano-particles at 0.60% (w/w) were below the friction factor of the base mud over time, although, only a marginal decrease was achieved. Further experiments are warranted to evaluate the lubricity of the mud samples at different temperatures both before and after aging to confirm if these nano-particles still could contribute to isolating heat in the lubricating film and show a decreasing trend.

Conclusions

An experimental study has been described to evaluate the rheological characteristics of water-based muds using nano-particles. Five mud samples were examined, namely ordinary base mud, two cases of titania nano-particle-doped water-based mud and two cases of silica nano-particle-doped base mud. Density, rheology (gel strength, apparent viscosity, shear stress) and lubricity (torque and coefficient of friction) properties have been quantified using a variety of devices. Both before aging and after aging scenarios have been studied and the influence of temperature in particular on rheology and lubricity characteristics examined in detail. The pertinent conclusions from the present study may be summarized as follows:

- A small enhancement in base mud density is caused with silica nano-particles with no tangible modification achieved with titania nano-particles. Before aging, titania nano-particles achieve greater viscosity than base mud or silica-doped mud which reduces viscosity.
- Before aging, titania nano-particles result in higher plastic viscosity (PV), yield point (YP) and apparent viscosity (AV) of the drilling mud, although a decreased yield point when the concentration is lower i.e., 0.20% (w/w) at 40 °C.
- Before aging, silica nano-particles generally result in a decrease in the yield point and apparent viscosity of the drilling mud, which may be related to superhydrophilic characteristics.
- Before aging, titania nano-particles achieve the highest efficiency (low plastic viscosity and a high yield point), whereas silica nano-particles showed the lowest efficiency.
- Before aging, higher values of gel strength are associated with titania and lower values with silica nano-particles, whereas the greatest increase in gel strength is with base mud. The introduction of titania in the base mud generates a *gel structure* quicker than the base mud over time.
- After aging, and before stirring, greater plastic and apparent viscosity is achieved for silica nano-particles *and lower* viscosities with the titania nano-particles.
- After aging and before stirring, titania nano-particles cause a reduction in the drilling mud yield point, whereas silica nano-particles cause the opposite effect.
- After aging and before stirring, the increase in gel strength in silica nano-particles relative to the base mud is less dramatic than before aging.
- After aging and stirring, the greatest viscosities are achieved with 0.60% (w/w) SiO_2, and the lowest are associated with the base mud without any nano-particles.
- Before aging, with regard to lubricity, titania nano-particles at a concentration of 0.60% (w/w) attained the best performance for torque (i.e., lowest torque) compared to the other mud samples, although, a significant reduction in torque was not measured.
- Before aging, silica nano-particles, at a concentration of 0.20% (w/w), produced torque readings close to those of the base mud although these values increased with time, i.e., worst torque performance.
- Before aging, torque and CoF of the base mud increases with temperature, whereas the addition of nano-particles in the base mud results in a decrease in torque and CoF with temperature indicating an increase in heat dissipation (improved thermal conductivity) with nano-particles.
- After aging, only titania nano-particles at 0.60% (w/w) achieved CoF magnitudes below the base mud values indicating a non-trivial enhancement in lubricity.
- In general, the results of the lubricity after the aging process were superior to those before aging.

The results generally indicate that based on properties measured before the aging process, titania nano-particles at a concentration of 0.60% (w/w) could be used as an additive to improve the rheological properties and lubricity of a drilling fluid, provided a stable formulation is achievable for long periods of time. In this regard, they offer some promise as robust additives for reducing the torque and drag in highly deviated and ERD wells where there is no presence of shale. Further investigations are required, however, to gain deeper insight into the performance of both silica and titania (and indeed other) nano-particles to confirm their potential benefits for drilling operations. The present investigation also provides some useful and much-needed rheological data for

Table 27 Properties of titanium oxide TiO_2 nano-particles (US Research Nanomaterials, Inc, 2016)

Titanium oxide (TiO_2) nano-particles	
Properties	
Purity	99.9%
Average particle size	30 nm
Specific surface area	35–60 m^2/g
Colour	White
Morphology	Near spherical
Bulk density	0.25 g/cm^3
True density	4.23 g/cm^3

Table 28 Properties of silicon dioxide SiO_2 nano-particles (US Research Nanomaterials, Inc, 2016)

Silicon dioxide (SiO_2) nano-particles	
Properties	
Purity	96.3%
Average particle size	20–30 nm
Specific surface area	130–600 m^2/g
Colour	White
Bulk density	< 0.10 g/cm^3
True density	2.4 g/cm^3

numerical and mathematical models and efforts for calibrating such models with computational fluid dynamic codes are presently under way. Furthermore, there is an extensive range of other metallic nano-particles which could be explored including silver, zinc, copper, etc. In addition, further studies must be conducted, e.g., field trials to establish if indeed the nano-particles work in full-scale operations. It is hoped that the present work will stimulate petroleum engineers working in the field to consider this.

Acknowledgements The authors are grateful to the reviewers for their insightful comments which have served to significantly improve the present article.

Funding This research did not receive any specific Grant from funding agencies in the public, commercial, or not-for-profit sectors.

Compliance with ethical standards

Conflict of interest The author(s) declared no potential conflicts of interest with respect to the research, authorship, and/or publication of this article.

Appendix

Properties of nano-particles used in the experiments (see Tables 27, 28).

References

Abdo J, Haneef MD (2013) Clay nano-particles modified drilling fluids for drilling of deep hydrocarbon wells. Appl Clay Sci 86:76–82

Ahmet S, Mustafa VK, Reha O (2013) Performance analysis of drilling fluid liquid lubricants. J Pet Sci Eng 108:64–73

Al-Yasiri MS, Al-Sallami WT (2015) How the drilling fluids can be made more efficient by using nanomaterials. Am J Nano Res Appl 3:41–45

Amanullah Md, Al-Arfaj MK, Al-Abdullatif Z (2011) Preliminary test results of nano-based drilling fluids for oil and gas field application. In: SPE drilling conference and exhibition, Amsterdam, The Netherlands, March 1–3 SPE/IADC 139534. https://doi.org/10.2118/139534-ms

Bég OA, Basir MFM, Uddin MJ, Ismail AIM (2017) Numerical study of slip effects on asymmetric bioconvective nanofluid flow in a porous microchannel with an expanding/contracting upper wall using Buongiorno's model. J Mech Med Biol 17(5):1750059. https://doi.org/10.1142/s0219519417500592

Behnamanhar H, Noorbakhsh SS, Maghsoudloojafari H (2014) Environmentally friendly water-based drilling fluid for drilling of water-sensitive formations. J Pet Gas Explor Res 4(4):60–71

Bu H, Sun J, Wang C, Bu P (2013) Rheological properties of polymer-gel drilling fluids at high temperature and pressure. Chem Technol Fuels Oils 48(6):449–458

Choi SUS (1995) Enhancing thermal conductivity of fluids with nanoparticles. Development of applications of non-Newtonian flows. ASME J Fluids Eng 66:99–105

Dantas APT, Leite RS, Nascimento RCAM, Amorim LV (2014) The influence of chemical additives in filtration control of inhibited drilling fluids. Braz J Pet Gas 8(3):097–108

Dingsøyr E, Pedersen E, Taugbøl K (2004) Oil based drilling fluids with tailor-made rheological properties: results from a multivariate analysis. Annu Trans Nord Rheol Soc 12:10–23

FANN (2016) http://www.fann.com/fann/products/supplies-and-reagents/lab-equipment-supplies/blenders-and-mixers/mixers-hb.page. Accessed 10 Dec 2017

Fazelabdolabadi B, Khodadadi AA, Sedaghatzadeh M (2015) Thermal and rheological properties improvement of drilling fluids using functionalized carbon nanotubes. Appl Nanosci 5(6):651–659

Gray GR, Darley HCH, Rogers WF (1980) Composition and properties of oil well drilling fluids. Gulf Publishing Company, Houston

Hughes B (1995) INTEQ. Drilling Engineering Workbook. Baker Hughes INTEQ, Houston, Texas, USA

Huminic G, Huminic A (2012) Application of nanofluids in heat exchangers: a review. Renew Sustain Energy Rev 16:5625–5638

Hung YH, Gu HJ (2014) Multiwalled carbon nanotube nanofluids used for heat dissipation in hybrid green energy systems. J Nanomater. https://doi.org/10.1155/2014/196074 **(Article ID: 196074)**

Hwang Y, Lee J, Lee J, Jeong Y, Cheong S, Ahn Y, Kim S (2008) Production and dispersion stability of nano-particles in nanofluids. Powder Technol 186(2):145–153

Jin L, Yue D, Xu Z-W, Liang G, Zhang Y, Zhang J-F, Zhang X, Wang Z (2014) Fabrication, mechanical properties, and biocompatibility of reduced graphene oxide-reinforced nanofiber mats. RCS Adv 4(66):303–35041

Kaloudis E, Papanicolaou E, Belessiotis V (2016) Numerical simulations of a parabolic trough solar collector with nanofluid using a two-phase model. Renew Energy 97:218–229

Kannaiyan K, Anoop K, Sadr R (2016) Effect of nano-particles on the fuel properties and spray performance of aviation turbine fuel. ASME J Energy Resour Technol 139(3):032201-1–032201-8

Lvov YM, Pattekari P, Zhang X, Torchilin V (2011) Converting poorly soluble materials into stable aqueous nanocolloids. Langmuir 27(3):1212–1217

Mostafavi V, Ferdous MZ, Hareland G, Husein M (2011) Design and application of novel nano drilling fluids to mitigate circulation loss problems during oil well drilling operations. J Clean Technology. ISBN:978-1-4398-8189-7

OFITE (2014) OFI Testing Equipment, Inc. http://www.ofite.com/products/product/43-mud-balance-4-scale-metal. Accessed 14 Dec 2017

Olatunde AO, Usman MA, Olafadehan OA, Adeosun TA, Ufot OE (2012) Improvement of rheological properties of drilling fluid using locally based materials. Pet Coal 54(1):65–75

Qu Y, Lai X, Zou L, Su Y (2009) Polyoxyalkyleneamine as shale inhibitor in water-based drilling fluids. Appl Clay Sci 44(3):265–268

Slawomir R, Zbigniew KB, Malgorzata U (2009) Study on the application of starch derivatives as the regulators of potassium drilling fluids filtration. Chem Chem Tech 3:107–202

Tian Y, Zhang X, Geng H-Z, Yang H-J, Li C, Da S-X, Lu X, Wang J, Jia S-L (2017) Carbon nanotube/polyurethane films with high transparency, low sheet resistance and strong adhesion for antistatic application. RSC Adv 7(83):53018–53024

Yang S, Hou Y, Zhang B, Yang XH, Zhang H, Zhao HJ, Yang HG (2014) Precisely controlled heterogeneous nucleation sites for TiO_2 crystal growth. CrystEngComm 16:7502–7506

Yang S, Huang N, Jin YM, Zhang HQ, Su YH, Yang HG (2015) Crystal shape engineering of anatase TiO_2 and its biomedical applications. CrystEngComm 17:6617–6631

Zakaria M, Husein MM, Harland G (2012) Novel nano-particle-based drilling fluid with improved characteristics. In: SPE international oilfield nanotechnology conference and exhibition, 12–14 June, Noordwijk, The Netherlands